Research Article

Characterization of taurine and its derivative binding to HSA using calorimetry and docking

Bingli Jiang[a], Yanrong Hu[a], Anran Zhao[a], Xuan Luo[a], Weigao Pan[a,b] and Cuiwu Lin[a*]

[a]School of Chemistry and Chemical Engineering, Guangxi University, Nanning, Guangxi, P. R. China
[b]Guangxi Botanical Garden of Medicinal Plants, Nanning, Guangxi, China
_____

ABSTRACT

To better understand the mechanism of drug binding to proteins, the binding properties of taurine and its derivative 2-phthalimido-ethanesulfonic acid (PESA) with human serum albumin (HSA) were investigated under physiological conditions by calorimetry, circular dichroism (CD) spectroscopy and molecular modeling. Based on the thermodynamic data, molar reaction enthalpy, reaction order (n) and the rate constant (k) were calculated, the kinetics equations of TAU and PESA binding to HSA were obtained; hydrogen bond force played a major role in the complexes; the reactions were spontaneous; binding sites of both complexes were one site. The results of CD spectroscopy showed that the conformation of HSA−TAU and HSA−PESA did not have any high-ordered structural change. Computational mapping revealed the details of their binding conformations.

Key words: taurine, HSA, calorimetry, circular dichroism, molecular modeling
_____

INTRODUCTION

Taurine (TAU, scheme 1) or 2-Aminoethanesulfonic acid is a sulphur containing free β-amino acid in mammals. Various physiological roles of TAU have been reported, including calcium modulation [1, 2], membrane stabilization [3], intracellular osmotic regulation [4], the regulation of protein phosphorylation, antioxidant agent [5, 6].TAU combination of *L*-carnitine has a synergistic inhibitory effect on the proliferation and osteoblastic differentiation of vascular smooth muscle cells (VSMCs) [7]. In endothelial cells, taurine variably inhibits apoptosis, inflammation, oxidative stress and cell death, while increasing NO generation [2, 3]. It is involved in variety of important physiological processes, although much progress has been made in discovering its enigmatic and many-sided biological role, scarce insight on the mechanisms of its actions is available. This manuscript is aimed at gaining more thermodynamics and kinetics information on the TAU and its derivative 2-phthalimido-ethanesulfonic acid (PESA)binding to HSA.

Calorimetry is a powerful probe of reaction pathways and mechanisms by virtue of providing high-quality kinetic data. *Microcalorimeter* provides on-line, quasi-continuous, and non-invasive measures of reaction rate [8]. With the microcalorimetry, Zhai and their team explored the antibiotic resistance in bacteria and reported the thermokinetic parameters of the imipenem hydrolysis with B1 subclasses metallo-β-lactamase CcrA from *Bacteroides fragilis*[9].Zhao and his co-workers investigated the effects of two ginsenosides Rg_1 and Rb_1 on splenic lymphocytes growth[10], Yang's group studied on inhibition of two cephalosporins on *Escherichia coli*[11], Kong *et al*. investigated *S. dysenteriae* and *Candida albicans* growth affected by berberine [12, 13]. On the other hand, Isothermal titration calorimetry (ITC) is able to directly measure the thermodynamic binding parameters of drug-protein interactions and has found growing use over the past decade[14-16].ITC directly estimates the binding thermodynamics through measurement of the energetics of molecular interactions at constant temperature. A series of data points representing the amount of heat released (exothermic) or absorbed (endothermic) per mole of injectant (usually the ligand) after each injection is plotted as a function of the molar ratio $[L_T]/[M_T]$ of the total ligand

concentration, $[L_T]$, and the total macromolecule concentration, $[M_T]$, to generate the binding isotherm (Fig. 1). The thermodynamic binding parameters are obtained through fitting binding isotherm to the nonlinear least-squares. The adjustable parameters in fits are ΔH (enthalpy change, in kcal·mol^{-1}), k_a (association constant, in M^{-1}), and n (number of binding sites per monomer of the (macro) molecule in the cell). So, ΔG, the free energy of binding (kcal·mol^{-1}), can be calculated by Van't Hoff equation. From the Gibbs free energy equation, $T\Delta S$ (the entropy of binding kcal·mol^{-1}) at the experimental temperature, can be determined [15, 17, 18].

EXPERIMENTAL SECTION

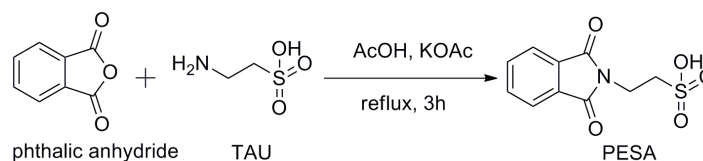### *Apparatus and reagents:*
Human Serum Albumin (HSA, Sigma–Aldrich) was dissolved daily in phosphate buffered saline (PBS: 150 mmol·L^{-1} NaCl, 2.7 mmol·L^{-1} KCl, 8.1 mmol·L^{-1}Na$_2$HPO$_4$, 1.9 mmol·L^{-1}KH$_2$PO$_4$, pH 7.4) to prepare a stock solution (2.0 × 10^{-4} mol·L^{-1}). Taurine (Sinopharm Chemical Reagent Co., Ltd.) PESA stock solutions (1 × 10^{-3} mol·L^{-1}) were prepared as follows: 0.025 mmol TAU or PESA, were dissolved in 25 mL of PBS (pH = 7.4).Other reagents were of analytical grade and used without further purification. Double distilled water was used for the experiments.

The thermogram was recorded by Microcalorimeter (RD496–CK2000, MianYang CP Thermal Analysis Instrument Co., Ltd). All pH measurements were made with a pHs–3C digital pH meter (Shanghai Leici Device Works, China) with a combined glass–calomel electrode.^{1}H and ^{13}C NMR spectra were recorded on a Bruker Advance III 300 at 300 MHz for ^{1}H and 75 MHz for ^{13}C, respectively in DMSO–d_6. Chemical shifts are given in δ (ppm) and coupling constants in Hz. ESI–MS was obtained on a Shimadzu LC–MS 2010A. ITC experiments were performed using an ITC200 Microcalorimeter from Micro Cal. The CD spectra of all mixtures were measured on anMOS–450 spectrometer (Bio–Logic, France).

Synthesis of 2-phthalimido-ethanesulfonic acid [19]
A suspension of taurine and anhydrous potassium acetate in acetic acid (AcOH) solvent was refluxed at 120 °C for 10 minutes, then phthalic anhydride was added (Scheme 1), and the reaction mixture was refluxed with stirring for additional 3 h. At the end of the reaction, a white precipitation was formed. After cooling in an ice-bath with continued stirring, the white product was filtered off, washed with acetic acid followed by alcohol, and purified by crystallization from water.

Scheme 1: Synthesis of 2-phthalimido-ethanesulfonic acid (PESA)

^{1}H NMR (300 MHz, DMSO-d_6) δ 7.87–7.80 (m, 4H, ArH), 3.85 (t, J = 7.8 Hz, 2H, CH$_2$), 2.77 (t, J = 7.8 Hz, 2H, CH$_2$), 2.52 (s, 1H, OH). ^{13}CNMR (75 MHz, DMSO-d_6) δ: 168.16(2C=O), 134.73(2C, aromatic), 132.23(2C, aromatic), 123.40(2C, aromatic), 49.10(CH$_2$), 34.93(CH$_2$). MS calcd [M – H]$^-$ for C$_{10}$H$_8$NO$_5$S 254.2, found 254.1.

Isothermal titration calorimetry (ITC)
HSA stock solution (5 × 10^{-5} mol·L^{-1}) was kept in ITC titration cell as a titer and was titrated by drug having a concentration of 1 × 10^{-3} mol·L^{-1}. Drug was injected through the computer-controlled 40 μL microsyringe at a successive time gap of 110 s between two injections into the HSA solution in the same buffer (cell volume = 200 μL) while stirring at 600 rpm. The experimental temperature was kept at 25°C.

Determination of thermodynamic parameters by microcalorimeter
The energy evolution was measured using a microcalorimeter. The structure and technical parameters of this calorimeter have been detailed previously [20]. The microcalorimeter was calibrated first using the Joule effect [20]. The calorimetric system was accurate (accuracy 0.02%) and reliable (precision 0.3%)[21, 22]. Drug solution (1.0 mL, 1 × 10^{-4}mol·L^{-1}) was placed in a small glass tube above the HSA (1.0 mL, 2.0 × 10^{-4}mol·L^{-1}), which was in a larger glass tube. After establishment of equilibrium, the small glass tube with drug solution was pushed down simultaneously. This led to mixing of the two solutions and the thermogram was recorded.

Circular dichroismspectra
One microlitre of HSA (1.0 × 10^{-5}mol·L^{-1}) and 1 μL drug (1.0 × 10^{-5}mol·L^{-1}) solutions was added into a 10 mL volumetric flask; PBS buffer was added to dilute the mixture to the scale mark. The CD spectra of all mixtures were measured on *circular dichroism* spectrometer. For measurements in the far–UV region (190–250 nm), a quartz cell

with a path length of 0.1 cm was used in nitrogen atmosphere.

Molecular modelling studies

The 2D structures of the TAU and PESA were drawn in ACD/ChemSketch (version 12.0), and then energy–minimized in PyRx Open Babel [23] using mm94 force field. The prepared structures were used as input file for the docking. The structure of HSA was taken from the Protein Data Bank having PDB ID: 1H9Z [24]. At the beginning of the docking study, warfarin and all water molecules were removed, In addition, polar hydrogens and Kollman charges were added, as required in the Lamarckian Genetic Algorithm. Grid maps of $232 \times 138 \times 231$ points with a grid–point spacing of 0.3750 Å were generated using the Auto Grid [25] in PyRx 0.8 (Local Execution Mode)[26-29]. The 200 genetic algorithm (GA) runs were performed with the following parameters: population size of 200, maximum number of 2.5×10^5 energy evaluations, maximum number of 27,000 generations.

RESULTS AND DISCUSSION
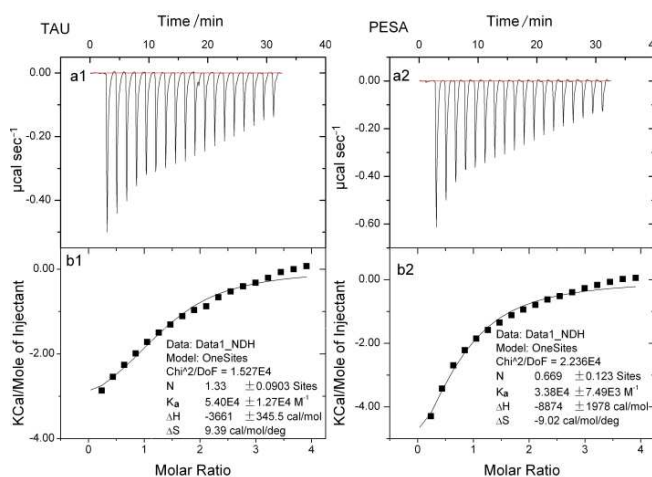
Thermodynamic Parameters from ITC

Fig. 1: ITC measurements of the binding of drug to HSA at 298K in phosphate buffer (pH = 7.4)
Parts a1 and a2 are the heat released during the titration of HSA (0.05 mM) by successive additions of a concentrated solution of TAU or PESA (1.0 mM), respectively; Figure parts b1 and b2 are the binding isotherms of TAU/HSA and PESA/HSA, respectively, after correction of heat for the dilution control; the solid line represents the best fit according to the independent model

The experimental data were fitted to a theoretical titration curve using the software supplied by Micro Cal. A standard one–site model was used with ΔH, K_a, and n as the variables. A typical titration is shown in Fig. 1a. The addition of drug solutions (1.0 mM) to the calorimeter cell which contained a solution of HSA (0.05 mM) resulted in the release of heat until the binding were saturated. The data must be corrected for the dilution heats associated with the addition of drugs into buffer solution. The area under each peak was integrated, heats of dilution are subtracted, and the thermograms for the binding of drugs to HSA have been obtained (Fig. 1b). The heats released during the binding were related to the number of binding sites available, binding constants and thermodynamic parameters of the binding equilibrium[30]. These data were best fitted to a single set of identical binding site model and yielding the binding parameters for drugswere given in Table 1. Additionally, the entropy and free energy of binding can be calculated.

Table 1: thermodynamic parameters of drug binding to HSA

drug	$K_a(M^{-1})$	$\Delta H(cal \cdot mol^{-1})$	ΔG (kcal·mol^{-1})	ΔS (cal·mol^{-1}·K^{-1})	n
TAU	5.40×10^4	−3661	−6.459	9.39	1.3
PESA	3.38×10^4	−8874	−6.186	−9.02	0.7

As can be seen, both ΔG values of TAU–HSA and PESA–HSA were negative, which revealed that the binding process was spontaneous. The negative value of $\Delta H$is frequently regarded as an evidence for hydrogen bond in the binding reaction. $\Delta S> 0$ observed in TAU experiment was mainly attributed to hydrophobic interactions. In addition, a specific electrostatic interaction between ionic species in an aqueous solution is characterized by apositive ΔS value and negative ΔH value [31]. So, in the binding of TAU to HSA process, hydrogen bond force most likely played a major role, but hydrophobic forces also could not be excluded. While in the binding of PESA to HSA process negative values of both ΔH and ΔS imply nonbonded (van der Waals) forces and hydrogen-bond formation [31]. The sites model of TAU binding to HSA was 1.3, and PESA binding to HSA was 0.7; they were approximately one site for interaction.

Kinetic investigation from microcalorimetry

The typical thermogram was obtained during the interaction of HSA and drug (Fig. 2). The energy change in the reaction depends on the reaction progress [32]. The reaction was initiated when the two liquids mixed, and the reaction between HSA and drug could be divided into three stages according to the thermogram. In the curve of HSA-TAU at 303.15 K (Fig. 2), there was an exothermic peak, dividing it into three stages, stage I: (0–76 s), stage II: (76–948 s), and stage III: (after 948 s); The same to PESA-HSA at 303.15 K (Fig. 2), the exothermic peak was also divided into three stages, stage I: (0–126 s), stage II: (126–997 s), and stage III: (after 997 s). Stage I: Reaction was triggered when the reagent solutions were mixed. Drug solution diffused and bound to HSA, which would contain dilution heat and reaction heat. Stage II: The solution was completely mixed and formed a uniform mixture; all of the heat flow was coming out of the heat of reaction. Stage III: The association–disassociation reached equilibrium, so the curve flattened and remained constant for about 3 h.
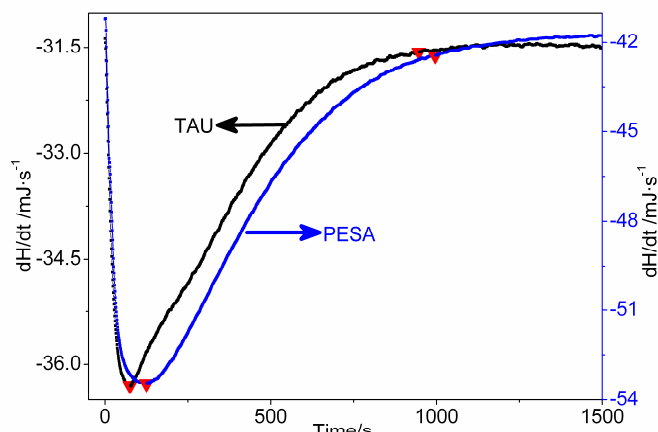

Fig. 2: Microcalorimetric heat flow curves of TAU and PESA binding to HSA

Equations 1 and 2 were chosen as the model function describing the time-dependent process of drug binding to HSA:

$$\frac{da_i}{dt} = kf(a_i) \tag{1}$$

$$f(a_i) = (1 - a_i)^n \tag{2}$$

Combining Eqs. 1 and 2 yields

$$\frac{da_i}{dt} = k(1 - a_i)^n \tag{3}$$

According to the reaction boundary conditions, the relationship between the reaction extent and the energy change in the reaction system, $a = H_i/H_\infty$, and then Eq. 3 can be expressed as

$$\frac{1}{H_\infty}\frac{dH_i}{dt} = k(1 - \frac{H_i}{H_\infty})^n \tag{4}$$

So, thermokinetic equation at constant temperature and pressure[33-35]was Eq. 5:

$$\ln(\frac{1}{H_\infty}\frac{dH_i}{dt}) = \ln k + n\ln(1 - \frac{H_i}{H_\infty}) \tag{5}$$

In the above equations, i is any time during the reaction process; α_i is the fraction of reaction at time i; $d\alpha_i/dt$ is the rate of reaction; $f(a_i)$ is the kinetic function; H_i represents the heat at time i; H_∞ is the heat of the whole process; (dH_i/dt) is the enthalpy change rate at time i, k is the rate constant; n is the reaction order.

Table 2: the reaction enthalpy, rate constant k and reaction order n of TAU and PESA binding to HSA

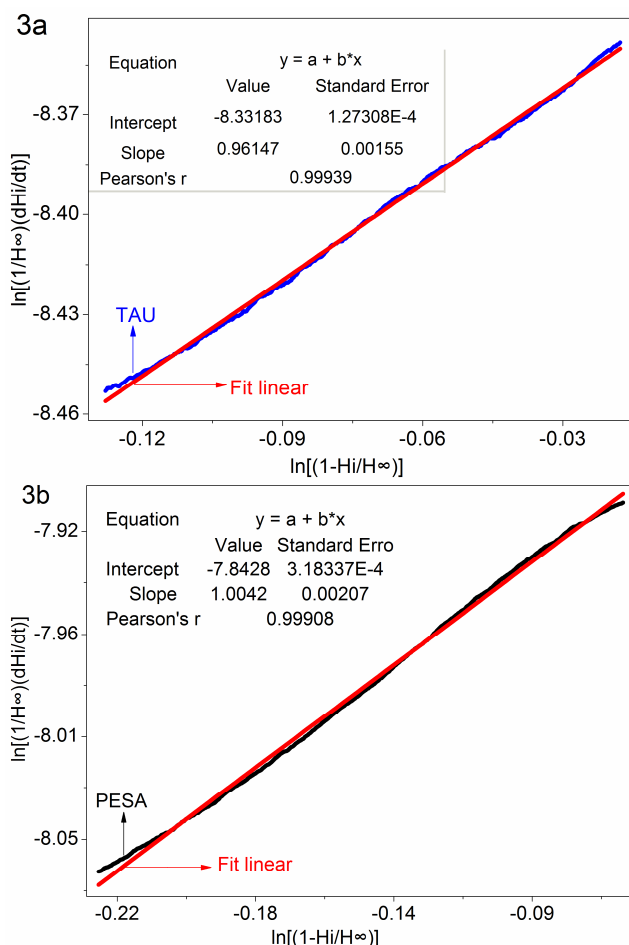|	H_∞(J)	ΔH_m(J·mol^{-1})	k	n
TAU–HSA	−33.251	−3.32× 10^5	2.41× 10^{-4}	0.96
PESA–HSA	−47.288	−4.72× 10^5	3.94× 10^{-4}	1.00

Fig.3: The plots of $ln[(1/H_\infty)(dH_i/dt)]$**versus** $ln[(1-H_i/H_\infty)]$**, (a) HSA−TAU; (b) HSA−PESA**

Based on the thermokinetic equations (5), the rate constant (k) can be obtained through linear regression analysis of stage II. lnk is the ordinate of the double logarithm regression curve of$ln[(1/H_\infty)(dH_i/dt)]$versus$ln[(1–H_i/H_\infty)]$ (Fig. 3) when $ln[(1– H_i/H_\infty)]$ is set at 0 and n is the slope of the curve. The curves exhibited a comparatively good linear relationship, the rate constant k and the reaction order n could be achieved from the figures and listed in Table 2. The reaction order $n$of both TAU and PESA binding to HSA were approximation to 1, which proved that the reaction process between TAU binding to HSA and PESA binding to HSA were similar to a quasi-first-order reaction.

Substituting the values of n and k into Eq. (3), we can get that the kinetics equation of TAU and PESA binding to HSA process is $d\alpha_i/dt = 10^{3.62} (1 − \alpha_i)^{0.91}$, $d\alpha_i/dt = 10^{3.41} (1 − \alpha_i)^{1.17}$, respectively.

Circular dichroism studies
Circular dichroism spectra can provide useful information of protein such as the content changes of the α-helix structure and secondary structure involving the β-sheet component [36].CD spectra of HSA with drug–HSAwere shown in Fig. 4. The native HSA exhibited two negative bands at 208 and 222 nm, which were characteristic of the typical α-helical structure of the protein. A reasonable explanation was that the negative peaks between 208–209 and 222–223 nm contributed to the $n \rightarrow \pi^*$ transfer for the peptide bond of α-helix [37, 38]. Furthermore, the fact that the 208 nm band was larger than that at 222 nm indicated that there was an $\alpha + \beta$ structure in native HSA[39]. The secondary structures of native HSA and drug–HSA were evaluated by comparing the α-helix contents, corresponding to the ellipticity of the bands at 208 nm. The CD results were expressed in terms of mean residue ellipticity (*MRE*) in deg·cm^2·d·mol^{-1} according to equation (6)[40]:

$$MRE = \frac{ObservedCD(medg)}{C_p nl \times 10}$$

(6)

Where $C_P$is the molar concentration of the protein, n is the number of amino acid residues (583) and l is the path length (0.1 cm). The α-helix contents of HSA can be calculated by the MRE value at 208 nm using equation (7):

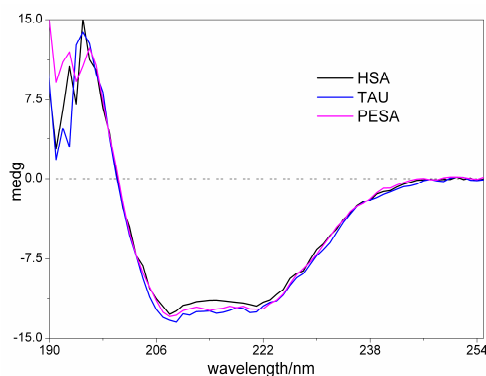$$aHelical(\%) = \frac{-MRE_{208} - 4000}{33000 - 4000} \times 100$$

(7)

Fig.4: CD spectra of free HSA and its TAU or PESA complexes: $C_{HSA} = 1.0 \times 10^{-6}$ **mol·L^{-1},** $C_{TAU}/C_{HSA} = C_{PESA}/C_{HSA} = 1:1$**, pH = 7.40, 298K**

Where MRE_{208} is the observed MRE value at 208 nm, 4000 is the MRE of the *β*-form and random coil conformation cross at 208 nm, and 33,000 is the MRE value of a pure *α*-helix at 208 nm.

With the above equation, the *α*-helix contents were obtained from CD spectra (Fig. 4). The intensity of the minimum reflects the amount of helicity of HSA. The calculated results exhibited a small increase in the *α*-helical content from 51.26%in free HSA to 53.01% in HSA–TAU and 52.15% in HSA–PESA, Which showed that the binding of TAU or PESA to HSA may induce minor conformational changes.TAU or PESA binding to the surface of HSA and some of functional groups inserting into the hydrophophobic surface of HSA and the electrostatic action according to the discussion in section 3.1 can stabilize the structure of HSA in solution, which explains the increasing *α*-helicity of HSA when bound to TAU. It also can be observed from Fig. 4 that the CD spectra of HSA in presence and absence of drugs were similar in shape in the region (190–250nm), which indicated that TAU or PESA did not cause any high-ordered structural change of HSA.

Docking analysis of TAU and PESA to HSA
The resulting conformations were clustered using a root-mean-square deviation (rmsd) of 2.0 Å and the clusters were ranked in order of increasing binding free energy of the lowest binding energy conformation in each cluster. The lower binding energy conformer was searched out of 50 different conformers for docking simulation, and the resultant one was used for further analysis MGL Tools[25] and LigPlot [41, 42] were used to visualize the docked conformations and calculate the distances between possible hydrogen bonding partners. The optimum binding mode and binding site were given in Fig. 5. The binding energies of TAU-HSA and PESA-HSA were listed in Table 3. The lowest binding energies of the conformations in clusters were –4.05 and –6.07 kcal·mol^{-1} for TAU–HSA and PESA–HSA complexes, respectively. These Gibbs free energies indicated that the interaction between TAU or PESA and HSA were highly spontaneous and energetically favorable.

Table 3: binding energy of drug and HSA (kcal·mol^{-1})

Binding Energy =(1)+(2)+(3)-(4)	Intermol Energy(1)	Internal Energy(2)	Torsional Energy(3)	Unbound Energy(4)
–6.07	–7.26	–0.79	1.19	–0.79
–4.05	–5.24	–0.81	1.19	–0.81

As shown in Fig. 5, the amino of TAU was adjacent to the acidic residues GLU153 and hydrophilic amino acid SER192, but the sulfonate group of TAU formed a hydrogen bond with basic amino acid ARG257 and HIS288. There was also hydrophobic interaction between the methylene and hydrophobic amino acids TYR150. This suggested that hydrogen bond most likely played a major role in the binding of TAU to HSA, and hydrophobic forces had also contributed. A little different binding mode was found in PESA, hydrophobic force, this is not unexpected because there was a difference of TAU and PESA. PESA has hydrophobic benzene, so the hydrophobic residues ALA191, ASN429, VAL433, TYR452 and VAL456 provide a hydrophobic pocket for the benzene of PESA. The H-bonding interactions were also involved in the binding of PESA to HSA, the PESA hydrogen atoms in the sulfonate group oriented toward the electron-rich oxygen in residue ASP187, sulfonate oxygen served as proton acceptors to form hydrogen bonds with amino hydrogen atom in residues LYS190 and LYS432. So in the binding of PESA to HSA process, the polar residues, as well as nonpolar amino acids, make major contributions to the binding of PESA, which means hydrophobic forces and hydrogen bond forces were the main interaction forces.
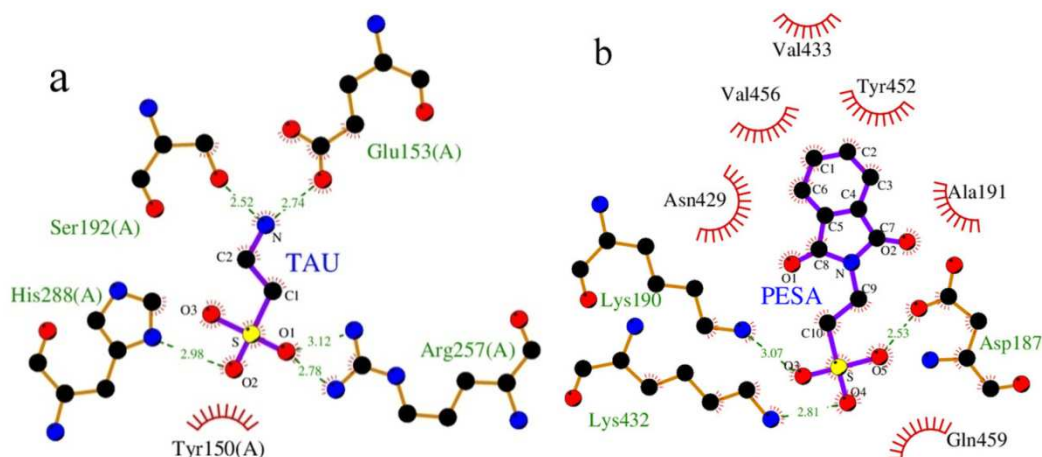
Fig. 5: Structural details of the interaction between TAU or PESA and HSA obtained by molecular modeling method
Ligands bonds are shown as purple; the ligands and amino acid residues are denoted as sticks and ball models (C, black; O, red; N, blue; S, yellow.) and the hydrogen bonds depicted by green dotted line, while the spoked arcs represent residues making nonbonded contacts with the ligand. The ligands are: (a) HSA−TAU. (b) HSA−PESA

CONCLUSION

In summary, in this work, the interaction of TAU and its derivative PESA with HSA were studied by calorimetry techniques, CD spectra and molecular modeling. Isothermal titration calorimetry results revealed that the both binding processes were spontaneous, HSA had one site for interaction with TAU or PESA. Thermodynamic data suggested hydrogen forces played a major role in the binding of TAU to HSA, while hydrophobic forces and hydrogen bond forces were the main interaction forces in HSA−PESA, which were in agreement with the docking results. The kinetics equation of TAU and PESA binding to HAS were also obtained from the microcalorimetry, it was $d\alpha_i/dt = 10^{-3.62} (1 - \alpha_i)^{0.91}$, $d\alpha_i/dt = 10^{3.41}(1 - \alpha_i)^{1.17}$, respectively. The CD spectra of HSA in the presence and absence of TAU or PESA were nearly identical, which meant that TAU or PESA did not cause any high-ordered structural change of HSA.

The kinetics and binding study of TAU and its derivative PESA with serum albumin are helpful for understanding their effects on protein function during their transportation and distribution in blood, which would provide primary information for research and development of new drug.

REFERENCES

[1] E Albiñana; S Sacristán; R Martín del Río; JM Solís; JM Hernández-Guijo. *Cellular and Molecular Neurobiology*, **2010**, 30(8), 1225-1233.
[2] S Schaffer; C Ju Jong; R KC; J Azuma. *J Biomed Sci*, **2010**, 17(Suppl 1), S2.
[3] W Abebe; MS Mozaffari. *Am. J. Cardiovasc. Dis.*, **2011**, 1(3), 293-311.
[4] JE Olson; E Martinho. *Journal of Neurochemistry*, **2006**, 96(5), 1375-1389.
[5] X Shao; Z Hu; C Hu; Q Bu; G Yan; P Deng; L Lv; D Wu; Y Deng; J Zhao; R Zhu; Y Li; H Li; Y Xu; H Yang; Y Zhao; X Cen. *Toxicol Appl Pharmacol*, **2012**, 260(3), 260-270.
[6] C Jong; J Azuma; S Schaffer. *Amino Acids*, **2012**, 42(6), 2223-2232.
[7] H Xie; B Yang; XM Zhou; FL Song; JM Li; K Zhou; W Hu; YQ Peng; SY Tang; LQ Yuan; SY Xiong; XB Liao. *Acta Pharmacol Sin*, **2010**, 31(3), 289-296.
[8] C LeBlond; J Wang; RD Larsen; CJ Orella; AL Forman; RN Landau; J Laquidara; JR Sowa Jr; DG Blackmond; YK Sun. *Thermochim Acta*, **1996**, 289(2), 189-207.
[9] L Zhai; KW Yang; CC Liu; HZ Gao; X Yang; Y Shi; J Wen. *Thermochim. Acta*, **2012**, 539(0), 67-70.
[10] YL Zhao; JB Wang; P Zhang; LM Shan; RS Li; XH Xiao. *J Therm Anal Calorim*, **2011**, 104(1), 357-363.
[11] L Yang; L Sun; F Xu; J Zhang; J Zhao; Z Zhao; C Song; R Wu; R Ozao. *J Therm Anal Calorim*, **2010**, 100(2), 589-592.

_____

[12] W Kong; Z Li; X Xiao; Y Zhao; P Zhang. *J Therm Anal Calorim*, **2010**, 102(1), 331-336.

[13] Y Zhao; D Yan; J Wang; P Zhang; X Xiao. *J Therm Anal Calorim*, **2010**, 102(1), 49-55.

[14] O Samsonova; S Glinca; A Biela; C Pfeiffer; E Dayyoub; D Sahin; G Klebe; T Kissel. *Acta Biomater*, **2013**, 9(2), 4994-5002.

[15] TK Dam; CF Brewer. *Chem Rev*, **2002**, 102(2), 387-430.

[16] T Cedervall; I Lynch; S Lindman; T Berggard; E Thulin; H Nilsson; KA Dawson; S Linse. *PNAS*, **2007**, 104(7), 2050-2055.

[17] S Leavitt; E Freire. *Curr Opin Struc Biol*, **2001**, 11(5), 560-566.

[18] JE Ladbury; BZ Chowdhry. *Chem Biol*, **1996**, 3(10), 791-801.

[19] O Akgul; FS Kilic; K Erol; V Pabuccuoglu. *Arch. Pharm. (Weinheim, Ger.)*, **2007**, 340(12), 656-660.

[20] M Ji; MY Liu; SL Gao; QZ Shi. *Instrum Sci Technol*, **2001**, 29(1), 53-57.

[21] YX Ren; SL Gao; SP Chen; BJ Jiao; RZ Hu; QZ Shi. *Chinese J Chem*, **2004**, 22(10), 1095-1101.

[22] Y Li; J Jiang; G Fan; Y Ma; Z Huang. *Chinese Sci Bull*, **2011**, 56(3), 269-274.

[23] NM O'Boyle; M Banck; CA James; C Morley; T Vandermeersch; GR Hutchison. *J cheminform*, **2011**, 3, 33.

[24] I Petitpas; AA Bhattacharya; S Twine; M East; S Curry. *J Biol Chem*, **2001**, 276(25), 22804-22809.

[25] MF Sanner. *J. Mol. Graph. Model.*, **1999**, 17(1), 57-61.

[26] O Trott; AJ Olson. *J. Comput. Chem.*, **2010**, 31(2), 455-461.

[27] DH Utomo; N Widodo; M Rifa'i. *Bioinformation*, **2012**, 8(9), 426-429.

[28] N Suvannang; C Nantasenamat; C Isarankura-Na-Ayudhya; V Prachayasittikul. *Molecules*, **2011**, 16(5), 3597-3617.

[29] RB Jacob; T Andersen; OM McDougal. *PLoS Comput Biol*, **2012**, 8(5), e1002499.

[30] T Yuan; AM Weljie; HJ Vogel. *Biochemistry*, **1998**, 37(9), 3187-3195.

[31] PD Ross; S Subramanian. *Biochemistry-US*, **1981**, 20(11), 3096-3102.

[32] L YanFen; J JunYing; F GaoChao; J Yu; H ZaiYin. *Chinese Sci Bull*, **2011**, 56(3), 269-274.

[33] W Ng. *Aust. J. Chem.*, **1975**, 28(6), 1169-1178.

[34] LD Hansen; EA Lewis; DJ Eatough; RG Bergstrom; D DeGraft-Johnson. *Pharmaceut. Res.*, **1989**, 6(1), 20-27.

[35] DN Waters; JL Paddy. *Anal. Chem.*, **1988**, 60(1), 53-57.

[36] Ap Zhu; Lh Yuan; T Chen; H Wu; F Zhao. *Carbohyd. Polym.*, **2007**, 69(2), 363-370.

[37] YJ Hu; Y Liu; XS Shen; XY Fang; SS Qu. *J. Mol. Struct.*, **2005**, 738(1–3), 143-147.

[38] XX Cheng; Y Lui; B Zhou; XH Xiao; Y Liu. *Spectrochim. Acta A*, **2009**, 72(5), 922-928.

[39] JT Pelton; LR McLean. *Anal Biochem*, **2000**, 277(2), 167-176.

[40] YZ Zhang; J Dai; XP Zhang; X Yang; Y Liu. *J. Mol. Struct.*, **2008**, 888(1-3), 152-159.

[41] AC Wallace; RA Laskowski; JM Thornton. *Protein Eng*, **1995**, 8(2), 127-134.

[42] RA Laskowski; MB Swindells. *J Chem Inf Model*, **2011**, 51(10), 2778-2786.